Turkish Journal of Physics

Volume 28 | Number 3 Article 4

1-1-2004

Analysis of One-Nucleon Transfer Cross-Sections

A. K. A. R. AL-FARRA

Follow this and additional works at: https://journals.tubitak.gov.tr/physics

 Part of the Physics Commons

Recommended Citation

AL-FARRA, A. K. A. R. (2004) "Analysis of One-Nucleon Transfer Cross-Sections," *Turkish Journal of Physics*: Vol. 28: No. 3, Article 4. Available at: https://journals.tubitak.gov.tr/physics/vol28/iss3/4

This Article is brought to you for free and open access by TÜBİTAK Academic Journals. It has been accepted for inclusion in Turkish Journal of Physics by an authorized editor of TÜBİTAK Academic Journals. For more information, please contact academic.publications@tubitak.gov.tr.

Turk J Phys
28 (2004) , 169 – 174.
© TÜBİTAK

Analysis of One-Nucleon Transfer Cross-Sections

Abdel Khaliq Abdel Rahman AL-FARRA
Physics Department, Faculty of Science, Al-Azhar University,
P.O. Box 1277, Gaza-PALESTINE
e-mail: a_a_farra@hotmail.com

Received 18.08.2003

Abstract

The angular distributions of $^{26}Mg(^3H,^2H)^{27}Mg$ and $^{30}Si(^3H,^2H)^{31}Si$ reactions have been successfully studied using distorted wave Born approximation (DWBA) calculations. The optical model potentials are taken to have Woods-Saxon, parity and spin-orbit interactions. The present analysis gives a satisfactory fit to the forward angle data but grossly over estimates the cross-sections in the backward regions. The spin-orbit potential provides the best description of the experimental data and is found to be necessary to account for the large-angle cross sections.

The obtained values of the extracted spectroscopic factors are reasonable.

1. Introduction

Over the years a number of theoretical calculations have been extensively introduced to explain the resonant structures which usually observed in heavy-ion transfer reactions. Following the microscopic DWBA calculations [1-3], the angular distributions of both (^3He, p) and (^3He, n) reactions have been reproduced reasonably well at energies below and above Coulomb barrier. The calculated differential cross-sections for ^{16}O(p,d)^{15}N reaction at 40.9 MeV[4] with excitation energies up to 12 MeV were noticeably improved through the using of both the DWBA calculations and cluster folding model. Interestingly, the measured cross-sections for the transitions to the ground and several-excited states in $^{26}Mg(^3He,\ n)^{28}Si$ reaction were found in reasonable agreement with the DWBA predictions [5]. In a ddition, the use of the coupled channel calculatios [6] explain the uprising oscillatory structures of various states up to 8 MeV excitation energy in the (^3He, n) reaction.

In the present work, the angular distributions of $^{26}Mg(^3H,\ ^2H)^{27}Mg$ and $^{30}Si(^3H,\ ^2H)^{31}Si$ reactions have been explored in terms of one-step DWBA calculations using various optical potential prescriptions. In Section 2, the phenomenological nuclear potential is introduced. Numerical calculations and results are given in Section 3. Section 4 is left for discussion and conclusion.

2. Nuclear Potential

In the present section, the differential cross sections of one-nucleon transfer reactions have been calculated in terms of one-step DWBA calculations using various nucleus-nucleus interactions [7–9]. The details of the present evaluation is given explicitly on the basis of the microscopic analysis [1]. For these calculations, the optical potential model was modified to include both a parity-dependent real potential and angular momentum absorptive term. The potential used has the form [7]

$$V(r) = [V(E_{c.m.}, \ell) \, + \, iW(E_{c.m.}, J)] \, f(r) + V^C(r), \tag{1}$$

where the Woods-Saxon form factor is given as

$$f(r) = \{ \, 1 + \exp \left[(r - R_i)/a_i \right] \, \}^{-1}; \quad i = V, \, W. \tag{2}$$

The depth of the real potential is taken to have the form

$$V(E_{c.m.}, \, \ell) = V_o + V_E \, E_{c.m.} + (-1)^{\ell} \, V_{\pi}, \tag{3}$$

where the values of the potential parameters are fixed at $V_o = -12.99$ MeV, $V_E = -0.62$MeV and $V_{\pi} = 0.69$MeV. The imaginary part is demonstrated by the superiority of J-dependent strength, given as

$$W(E_{c.m.}, \, J) = (W_o + W_E \, E_{c.m.}) \, \{ \, i + \exp \left[(J - J_c)/\Delta J \right] \, \}^{-1}, \tag{4}$$

where W_o and W_E describe an energy dependent absorptive potential. J_c is the cut-off angular momenta [7] and ΔJ is the angular momenta cut-off diffuseness parameter.

3. Numerical Calculations and Results

To show the sensitivity of the optical potential in reproducing the single nucleon transfer data, the differential cross sections have been numerically carried out for ^{26}Mg, $^{30}Si(^3H, \, ^2H)$reactions at 36 MeV. In a first set of calculations, the optical potential is assumed to have a standard Woods-Saxon potential [8]. As real and imaginary Woods-Saxon form factors give a satisfactory fit to the$^{26}Mg(^3H,^2 H)^{27}Mg$forward angle data but grossly over estimate the cross-section magnitudes at the backward region, the six-potential parameters were varied to give the best fit to the data by minimizing χ^2 as

$$\chi^2 = \frac{1}{N} \sum_{i=1} \frac{\left(\sigma^i_{\exp} - \sigma^i_{theor} \right)^2}{\left(\Delta \sigma^i_{\exp} \right)^2}, \tag{5}$$

where i is the summation index over N data points. The results obtained are found not to be significantly different from those results obtained with parameters used to start searches. In general, calculations using Woods-Saxon potentials have led to as similar results as those obtained in previous DWBA calculations [10]; and it is found that more than one potential parameter sets introduce good fits to the 1.67 MeV and 1.94 MeV states. The resulting parameters are listed in Table 1 and the fits to the data are shown in Figure 1 by dashed lines.

In a second set of optical model calculations, it is found that the fits to the $^{26}Mg(^3H, \, ^2H)^{27}Mg$ data with parity-dependent potential [7] are of very similar quality to those obtained using Woods-Saxon potential, as shown in Figure 1 by dash-dot curves. In view of the comparison, although calculations using both of parity and Woods-Saxon potentials were found not to be significantly different in the forward regions, employing the parity dependent potential leads to a substantially better description of the large angle cross sections.

Table 1. Optical potential parameters.

Channel	Data Set	$V_\circ$ (MeV)	r_v (fm)	a_v (fm)	$W_\circ$ (MeV)	r_w (fm)	a_w (fm)
^{2}H + ^{27}Mg	i	82.66	1.17	0.65	11.54	1.32	0.74
	ii	90.0	1.15	0.59	17.60	1.26	0.83
	iii	100.0	1.27	0.61	15.80	1.19	0.79
^{3}H + ^{26}Mg	i	108.4	1.16	0.76	20.11	1.65	0.74
	ii	120.0	1.29	0.69	24.20	1.35	0.66
^{3}H + ^{30}Si	i	128.10	1.07	0.80	15.52	1.74	0.67
	ii	95.0	1.19	0.63	23.60	1.24	0.85
	iii	86.0	1.35	0.71	18.40	1.41	0.76
^{2}H + ^{31}Si	i	83.60	1.17	0.65	11.54	1.74	0.67
	ii	92.0	1.08	0.79	17.80	1.45	0.81
	iii	98.0	1.12	0.69	16.20	1.49	0.73

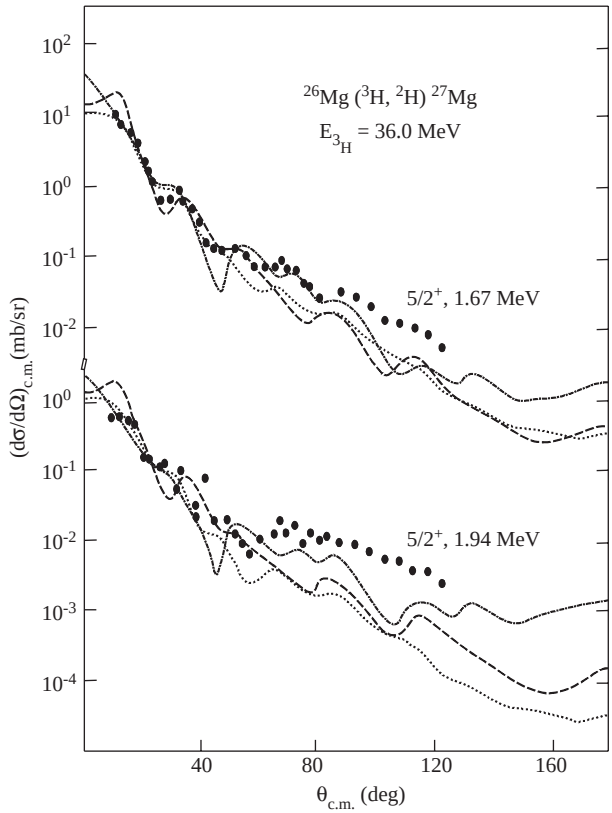

Figure 1. The angular distributions of $^{26}Mg(^3H,^2H)^{27}Mg$ reaction at 36.0 MeV. The line denoted by "– • – " (dash-dot-dash) and "– –" (dashed) lines show DWBA calculations using parity interaction and Woods-Saxon potential, respectively. The dotted lines ("• • •") show the previous DWBA calculations and the large dots denote the experimental data taken from Ref. [10].

To improve the quality of fits, another set of numerical calculations have been performed using the spin-orbit potential [9]. In this type of analysis, the wave functions by Cohen and Kurath (CK) was used for the positive-parity states in ^{31}Si[11], together with the Cohen and Kurath interaction [12] for the p-shell.

The phases and normalization's of the spectroscopic amplitudes obtained from these wave functions were carefully checked to make them consistent with the finite-range codes [13, 14]. From the results shown in Figure 2 by solid curves, it is clear that calculations using spin-orbit potential reproduce the differential cross sections reasonably well in the whole angular range. In such calculations, the bound-state potential is expressed to have a Thomas-Fermi spin-orbit of the form

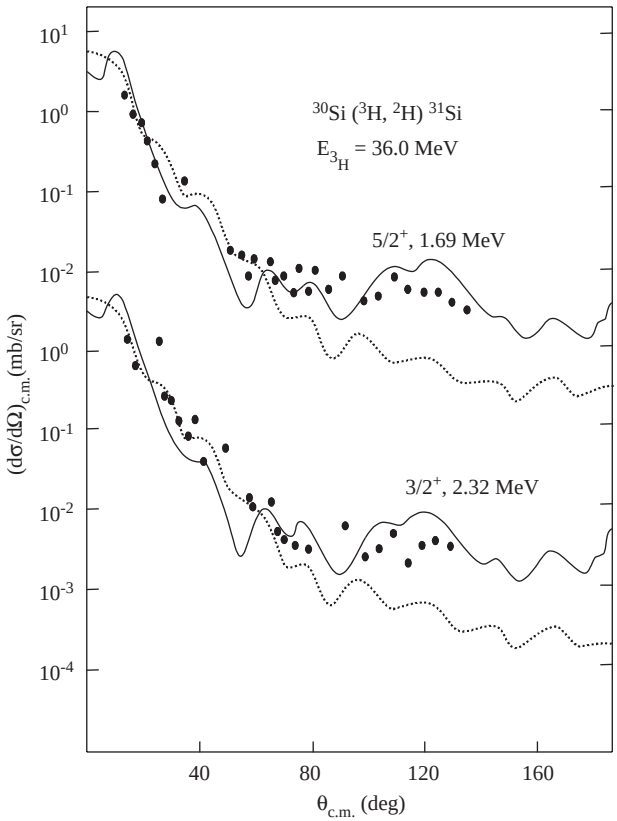

Figure 2. The angular distributions of $^{30}Si(^{3}H,^{2}H)^{31}Si$ reaction at 36.0 MeV. The solid lines show the present DWBA calculations using spin-orbit interaction. The dotted lines show the previous DWBA calculations and the data taken from Ref. [10].

$$V_{S.O.} = \frac{\lambda}{45.2}\frac{1}{r} f\left(r,\ r_{S.O.},\ a_{S.O.}\right). \tag{6}$$

with $\lambda = 25$ and the well depth of the real potential adjusted to give each nucleon separation energy. In the present calculations, the form factor of the transferred particle was calculated using the standard separation energy method in a Woods-Saxon well with $r_o = 1.25$fm, $a = 0.65$fm and spin-orbit strength $V_{LS} = 6$MeV. The depth is adjusted to reproduce the binding energy of the last nucleon and the number of nodes $N$for the radial wave function are fixed using the harmonic oscillator relation.

$$2N + L = \sum_i (2n_i + \ell_i) \tag{7}$$

where n_i and ℓ_i are the number of nodes and orbital angular momenta of transferred particle with respect to the core, respectively. By matching the results of the present DWBA calculations with the experimental data, the spectroscopic factors S_{ij} for each state is given as

$$\frac{(d\sigma/d\Omega)_{exp}}{(d\sigma/d\Omega)_{DWBA}} = \frac{1}{(2J+1)} N_D C^2 S_{ij}, \tag{8}$$

where N_D is the overall normalization constant and C^2 stands for the isospin factor. The obtained values of the spectroscopic factors are contained in Table 2.

Table 2. DWBA Spectroscopic factors.

Reaction	Excitation Energy (MeV)	J^π	Spectroscopic Factors				
			Previous [ref.10]		Present		
			a)	b)	*WS*	V_π	S.O.
^{26}Mg (^{3}H, ^{2}H) ^{27}Mg	1.67	$5/2^+$	0.04	0.06	0.56	0.67	0.79
	1.94	$5/2^+$	0.005	0.006	0.51	0.64	0.81
^{30}Si (^{3}H,^{2}H) ^{31}Si	1.69	$5/2^+$	0.03	0.04	0.61	0.66	0.83
	2.32	$5/2^+$	0.044	0.049	0.58	0.70	0.78

a) ZR-DWBA [11]
b) EFR-DWBA [11]

4. Discussion and Conclusion

In the present work, the differential cross sections of $^{26}Mg(^3H,^2H)^{27}Mg$ and $^{30}Si(^3H,^2H)^{31}Si$ reactions have been calculated reasonably well using simple one-step DWBA calculations. As shown in Figures 1 and 2, it is clear that the fits to the 36 MeV data are quite good against different optical potentials. From the dashed lines results shown in Figure 1, it is seen that the fits to $^{26}Mg(^3H,^2H)^{27}Mg$ large angle data within Woods-Saxon potential was noticeably poorer and not significantly different from those shown by the dotted lines. Interestingly, calculations using parity potential exhibit qualitative similar fits to the forward angle data and deviated significantly from the data at backward regions. In an attempt to find a more consistent analysis of the data, another overall fit to the $^{30}Si(^3H,^2H)^{31}Si$ data was obtained using a spin-orbit potential, and is shown in Figure 2 by solid curves. Use of the spin-orbit potential gives the best fit to the 36 MeV data and provides a much better description of the large angle cross sections than Woods-Saxon and parity forms. In view of comparison, although the parity potential is found to be reasonable in explaining the large angle data but a somewhat better description of the data is obtained within spin-orbit potential, where the calculated cross sections are an order of magnitude smaller for parity potential than spin-orbit one. Generally, one finds that the forward oscillatory structures are found to be nearly stable through using of the different potential types, while those at backward angles are greatly affected. Therefore, it is difficult to favor one of the potential used here over the other two in describing the forward angle data at 36 MeV. It is found that the various potential parameter sets together with different spectroscopic factors introduce qualitatively good results. In addition, the best fit to the 1.67 MeV and 1.94 MeV states were found with 15×10^4 MeV^2·fm^3 normalization factor, while 15×10^4 MeV^2·fm^3 and 20×10^4 MeV^2·fm^3 seem to be somewhat superior in reproducing both the ($5/2^+$; 1.69MeV) and ($3/2^+$; 2.32MeV) states, respectively.

For the ($5/2^+$; 1.67MeV) state, the calculated cross-section within parity-dependent potential is found to be smaller than the experimental measurements by 15% , while 10% smaller was predicted for the ($5/2^+$; 1.69MeV) state using spin-orbit potential.

In conclusion, the present DWBA calculations show a satisfactory fit to the 36 MeV one-nucleon transfer data. Since the calculated cross sections doesn't change appreciably with the potential type in the forward region, while the large angle data are extremely sensitive to the potential used. The inclusion of spin-orbit term is found to be reasonable to account for both shapes and magnitudes of the differential cross section.

References

[1] M. Haque, S.K. Das, A.K. Basak and H.M. Sen Gupta, *IL Nuovo Cimento*, **111A**, (1998), 1131.

[2] J. Vernotte, G. Berrier Ronsin, S. Fortier, E. Hourani, J. Kalifa, J. M. Maison, L. H. Rosier, G. Rotbard and B.H. Wildenthal, *Phys. Rev.*, **C48**, (1993), 205.

[3] H.M.Sen Gupta, J.B.A England, F.Khazaie, E.M.E Raways and G.T.A. Squier, *Nucl. Phys.,* **A5170**, (1990), 82.

[4] J.R. Campell, O.A. Abou-Zeid, W.R. Falk, R. Abegg, S.K. Datta, S.L. Datta and S.P. Kwan, *Nucl. Phys.*, **A467**, (1987), 205.

[5] K. Abe, K. Maeda, T. Ishimatsu, T. Kawamura, T. Furukawa, H. Orithara and H. Ohnuma, *Nucl. Phys.*, **A466**, (1987), 109.

[6] K. Abe, K. Maeda, T. Ishimatsu, T. Kawamura, T. Furakawa, H. Orithara and C.D. Zafirators, *Nucl. Phys.*, **A462**, (1987), 358.

[7] Y. Kondo, B. A. Robson, R. Smith and H. H. Wolter, *Phys. Lett.,* **B162**, (1985), 39.

[8] C. Tenreiro, J.C. Acquadro, P.A.B. Freitas, R. liguori Neto, G. Ramirez, N. Cuevas, P.R.S. Gomes, R. Cabezas, R.M. Anjos and J. Copnell, *Phys. Rev.,* **C5,** (1996), 2870.

[9] F.R. Andrewas, B.M. Spicer, G.G. Shute, V.C. Officer, J.M.R. Wastell, H. Nann, A.D. Bacher, D.L. Friesel and W. P. Jones, *Nucl. Phys.,* **A468**, (1987), 43.

[10] K.I. Pearce, N.M.Clarke, R.J. Griffithas, P.J. Simmonds, D. Barker, J.B.A. England, M. C. Mannion and C.A. Ogilvie, *Nucl. Phys.*, **A467**, (1987), 215.

[11] S. Cohen and D.kurath, *Nucl. Phys.*, **A101**, (1967),1.

[12] S. Cohen and D.Kurath, *Nucl. Phys.*, **A73**, (1965),1.

[13] T. Tamura, T. Udagawa, K.W. Wood and H. Amakawa, *Comp. Phys. Commun.*, **18**, (1979), 163.

[14] M.J. Rhoades-Brown, S.C. Pieper and M. Mac Farlane, *Phys. Rev.*, **C2,** (1980), 2436.